Bull. Chem. Soc. Ethiop. **2025**, 39(3), 437-446.
DOI: https://dx.doi.org/10.4314/bcse.v39i3.4

ISSN 1011-3924
Printed in Ethiopia
Online ISSN 1726-801X

A Cu(II) COORDINATION COMPOUND CONSTRUCTED BY MIXED LIGANDS OF 1,10-PHENANTHROLINE AND CARBOXYLIC ACID: SYNTHESIS, CHARACTERIZATION AND HIRSHFELD SURFACE ANALYSIS

Huilin Wang[1,2], Keming Liu[2], Zhiguo Kong[1,2], Lina Zhao[1,2*], and Hua Zhang[1,2]

[1]Key Laboratory of Preparation and Applications of Environmental Friendly Materials, Jilin Normal University, Ministry of Education, Changchun 130103, China
[2]Department of Chemistry, Jilin Normal University, Siping 136000, China

(Received April 3, 2024; Revised November 6, 2024; Accepted November 11, 2024)

ABSTRACT. Synthesis and full characterization of a new coordination compound, which was synthesized by mixed ligands under hydrothermal condition, namely $[Cu(L)_2(phen)_2(H_2O)_2]\cdot 4H_2O$ (**1**) (phen = 1,10-phenanthroline, H_2L = 3-carboxy-1-carboxymethyl-2-oxidopyridinium). Cu(II) is six-coordinated in a slightly twisted $[CuN_2O_4]$ octahedral geometry. **1** displays 2D supramolecular layer, which is further extended into a 3D network by the π-π stacking and hydrogen bonds. 3D Hirshfeld surface analysis is combined with 2D fingerprint plots to investigate the contribution of different intermolecular interactions within the crystal. DFT calculations are also performed.

KEY WORDS: Cu(II), 1,10-phenanthroline, Coordination compound, Hirshfeld surface analysis, DFT calculation

INTRODUCTION

The rational design and assembly of coordination compounds have gained a lot of attention of chemists in recent years because of their diverse topologies and potential applications in electrochemistry, photochemistry, adsorption, etc. [1-6]. However, there are many factors that influence the structure of coordination compounds, including coordination geometries of metal ions, organic ligands, solvent, reaction conditions, and reaction environment [7-8]. Among these mentioned influences, the selection of suitable organic ligands plays a crucial role in the synthesis of coordination compounds with interesting topologies [9-10]. It is well known that coordination covalent bonds and weak intermolecular forces are two important interactions for constructing coordination compounds, especially hydrogen bonding and π-π interactions among the weak intermolecular forces [11-14]. The rational use of weak intermolecular interactions to construct multidimensional coordination compounds is an important aspect of designing coordination compounds [15-16]. Thus, aromatic carboxylic acid ligands are widely applied in the construction of coordination compounds and they can act as both donors and acceptors of hydrogen bonds depending on the amount of deprotonated carboxylic acid [17-18]. For example, 3-carboxy-1-carboxymethyl-2-oxidopyridinium, which not only can serve as H-bonds acceptors and donors, but also can coordinate with metal ions in a variety of coordination modes [19]. In addition, the introduction of bidentate N-donor ligands such as 1,10-phenanthroline, used with aromatic carboxylic acid ligands can produce more exciting coordination structures and can generate π-π interactions, resulting in increasing the coordination compounds stability [20-23].

On the basis of the aforementioned points, we have synthesized a new Cu(II) coordination compound with H_2L and 1,10-phenanthroline, namely $[Cu(L)_2(phen)_2(H_2O)_2]\cdot 4H_2O$ (**1**). The structure and properties of **1** have been characterized, Hirshfeld surface analysis and DFT calculations have been carried out for **1**.

*Corresponding authors. E-mail: zhaolnjlnu@163.com

EXPERIMENTAL

Materials and measurements

All reagents and solvents are commercially available and do not require further purification for use in our laboratory. Elemental analyses (C, H, and N) of the solid **1** were determined Perkin-Elmer 240 CHN elemental analyzer (Perkin-Elmer, North Waltham, USA). Powder X-ray diffraction (PXRD) data was recorded on Bruker D8 Advance with Cu-*Kα* (λ = 1.54056 Å) radiation. Thermogravimetric analyses (TGA) was completed on a Perkin-Elmer TG-7 analyzer under N_2 from 25 to 800 °C. UV-Vis spectra was obtained at ambient temperature using a Shimadzu UV-2550 dual beam spectrophotometer. Hirshfeld surface analysis and related 2D fingerprints were performed with CrystalExplorer software version 21.5.

X-Ray single crystal structure determination

Suitable size of **1** was selected and crystal data were collected on Bruker-AXS Smart CCD diffractometer equipped with graphite monochromatic Mo-*Kα* radiation (λ = 0.71073 Å) at 293(2) K by using an *ω*-*ϕ* scan. The crystal structures were done by direct methods with SIR2014 [24] and refined with SHELXL2018/3 [25] by Least-Squares minimization on F^2. All H atoms were generated geometrically and are isotropically refined using a riding model. The results of single crystal X-ray diffraction analysis are summarized in Table 1. Some of the selected bonds lengths and angles are listed in Table 2.

Table 1. Crystalline data and refinement parameters for compound **1**.

Formula	$C_{40}H_{38}Cu_2N_6O_{16}$
M_r (g.mol^{-1})	985.84
Crystal system	Monoclinic
Space group	*P2₁/n*
a, b, c [Å]	11.928(5), 12.963(5), 12.803(5)
α, β, γ (°)	90, 91.497(5), 90
V (Å^3)	1979.0(14)
Z	2
ρ (g.cm^{-3})	1.654
μ (mm^{-1})	1.160
F(000)	1012
Crystal size (mm)	0.224 x 0.205 x 0.178
Temperature (K)	293(2)
Mo *Kα* radiation, λ (Å)	0.71073
θ (min-max) (°)	2.236, 26.403
Data set	-6<=h<=14, -16<=k<=16, -15<=l<=16
Tot., Unique data, R_{int}	11036, 4039, 0.0220
Observed [I>2σ(I)] reflections	3460
*N*reflections, *N*parameters	4039, 289
$R[F^2>2\sigma(F^2)]$, $wR(F^2)$, *S*	0.0346, 0.0973, 1.035
$\Delta\rho_{min}$, $\Delta\rho_{max}$ (e.Å^{-3})	-0.376, 0.417

Table 2. Selected bond lengths (Å) and angles (°) for the compound **1**.

Bond lengths (Å)			
Cu(1)-N(1)	2.0114(19)	Cu(1)-O(3)	1.9333(16)
Cu(1)-N(2)	1.9988(20)	Cu(1)-O(4)	1.9029(16)
Cu(1)-O(1W)	2.2855(18)	Cu(1)-O(5)^{i}	2.9165(11)
Bond angles (°)			
O(4)-Cu(1)-O(3)	93.43(6)	N(2)-Cu(1)-N(1)	82.18(8)
O(4)-Cu(1)-N(2)	169.55(7)	O(4)-Cu(1)-O(1W)	90.09(6)
O(3)-Cu(1)-N(2)	92.76(7)	O(3)-Cu(1)-O(1W)	98.46(6)
O(4)-Cu(1)-N(1)	90.21(7)	N(2)-Cu(1)-O(1W)	97.31(6)
O(3)-Cu(1)-N(1)	168.75(7)	N(1)-Cu(1)-O(1W)	92.17(6)
O(3)-Cu(1)-O(5)^{i}	88.80(5)	N(1)-Cu(1)-O(5)^{i}	80.76(5)
O(4)-Cu(1)-O(5)^{i}	87.00(5)	N(2)-Cu(1)-O(5)^{i}	84.72(5)

Symmetry transformations used to generate equivalent atoms: ^{i} -*x*+2, -*y*, -*z*+1.

*Synthesis of **1***

A mixture containing $CuCl_2 \cdot 2H_2O$ (0.1mmol, 0.0170 g), H_2L (0.06 mmol, 0.0112 g) and 1,10-phenanthroline (0.1 mmol, 0.0186 g) was dissolved in 5 mL of DMF-H_2O (1:1 V/V) and placed in 15 mL vial and sealed. Then, it was heated at 92 °C for 4 days under autogenous pressure and cooled to room temperature at the rate of 5 °C/h. Blue crystals of **1** were collected. Yield 43% based on Cu. Anal. calcd. for $C_{40}H_{38}Cu_2N_6O_{16}$ (FW 985.84): C, 48.73; H, 3.89; N, 8.52. Found: C, 47.92; H, 3.83; N, 8.42.

RESULTS AND DISCUSSION

Powder X-ray diffraction (PXRD) and IR spectroscopy

The simulated and measured PXRD patterns of **1** are depicted in Figure 1a. It can be seen that the measured PXRD pattern of **1** is almost identical to the simulated one, indicating the purity of the bulk powder samples of **1**. In the IR spectrum (Figure 1b), O–H stretching vibrations for water molecules is strong and wide with the peak at about 3368 cm^{-1}. Two peaks at 1587 and 1374 cm^{-1} could be ascribed to the anti-symmetric stretching and the symmetric stretching vibrations of coordinate carboxylates of L anion. The adsorption peaks of coordinate phen ligand are located at 1648, 1429, 854 and 724 cm^{-1}.

Thermogravimetric analyses

Thermogravimetric analysis (TGA) was clarified to study thermal stability of **1** at 25-800 °C under N_2 atmosphere with the temperature increase rate of 10 °C/min. As depicted in Figure 2a, the first weight loss of 10.9 % from 26 to 170 °C, which is attributed to the departure of two coordinated water molecules and four free water molecules (calcd. 11.0%). The second weight loss can be corresponded to the decomposition of both phen ligands and the organic group $C_8H_5NO_4$ of L anions in the temperature range of 202-539 °C (obsd. 72.7%, calcd. 72.9%), result in the formation of CuO as the residue (obsd. 16.4%, calcd. 16.1%).

UV-Vis absorption spectra

The UV-Vis absorption spectra of **1** was performed in the crystalline state at room temperature. The energy bands of **1** from 470 to 800 nm are designated as d-d transitions, while lower energy bands from 200 to 440 nm for **1** are considered as intraligand transitions [26]. The above analysis is consistent with the crystal structure determination (Figure 2b).

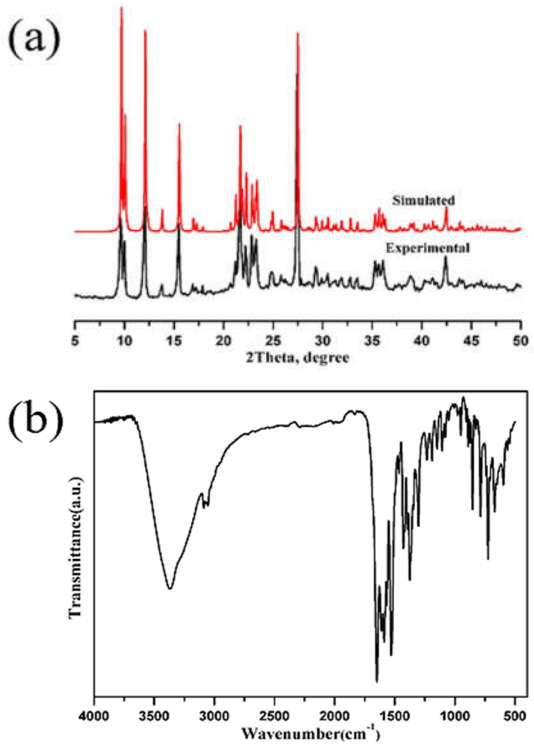

Figure 1. (a) Experimental and simulated PXRD patterns of **1**; (b) IR spectrum of complex **1**.

Crystal structure

The asymmetric unit of **1** is composed of one Cu(II) atom, one L anion, one 1,10-phenanthroline, one coordinated water, and two crystal waters. As seen in Figure 3a, each Cu(II) cation is six-coordinated by two nitrogen atoms (N(1) and N(2)) are from one chelating phen (Cu(1)–N(1) = 2.0114(19), Cu(1)–N(2) = 1.9988(20) Å), and four oxygen atoms (O(3), O(4), O(5^{i}) and O(1W)) from two L anions and one coordinated water (Cu(1)–O(3) = 1.9333(16), Cu(1)–O(4) = 1.9029(16), Cu(1)–O(5^{i}) = 2.9165(11) and Cu(1)–O(1W) = 2.2855(18) Å) in a slightly twisted [CuN_2O_4] octahedral geometry. The Cu(II) cation exhibits strong Jahn–Teller distortion with the Cu(1)–O(5^{i}) bond distance of 2.9165(11) Å. Cu(1) and the symmetry formed Cu(1^{i}) cations are linked with two chelating-bridging-tridentate phenolic hydroxyl and carboxylate groups from two independent L anions to yield a binuclear unit. The Cu···Cu separation by L anions is 5.135 Å. As illustrated in Figure 3b, owing to the presence of aromatic phen and L anion, contiguous $[Cu(L)_2(phen)_2(H_2O)_2]\cdot 4H_2O$ molecules are formed into a supramolecular layer by π-π stackings between phen and pyridine of L anion (Figure 3c, Table 3). More interestingly, there exist the O–H···O hydrogen bonds (H(1A)···O(2^{v}) = 1.92, O(1W)···O(2^{v}) = 2.740(3) Å, ∠ O(1W)–H(1A)···O(2^{v}) = 164.5°, symmetric code: ^{v} -*x*+3/2, -*y*+1/2, -*z*+3/2.), which further prompt the neighboring two-dimensional layers to grow up into a three-dimensional supramolecular structure (Figure 3d). Additionally, π-π interactions (Cg3···Cg5^{i}, Cg4···Cg4^{iii} and Cg4···Cg8^{iii}, symmetric code: ^{i} -*x*+2, -*y*, ^{iii} -*x*+1, -*y*, -*z*+1, as seen in Table 3 and O–H···O hydrogen bonds (O(1W)-

H(1B)···O(3W), O(2W)-H(2A)···O(4), O(2W)-H(2A)···O(5), O(2W)-H(2B)···O(1)^{i}, O(3W)-H(3A)···O(2)^{vi} and O(3W)-H(3B)···O(2W), symmetric code: ^{i} -*x*+2, -*y*, -*z*+1, ^{v} -*x*+3/2, *y*+1/2, -*z*+3/2, ^{vi} *x*+1/2, -*y*+1/2, *z*-1/2, as seen in Table 4 further reinforces the three-dimensional supramolecular structure of **1**.

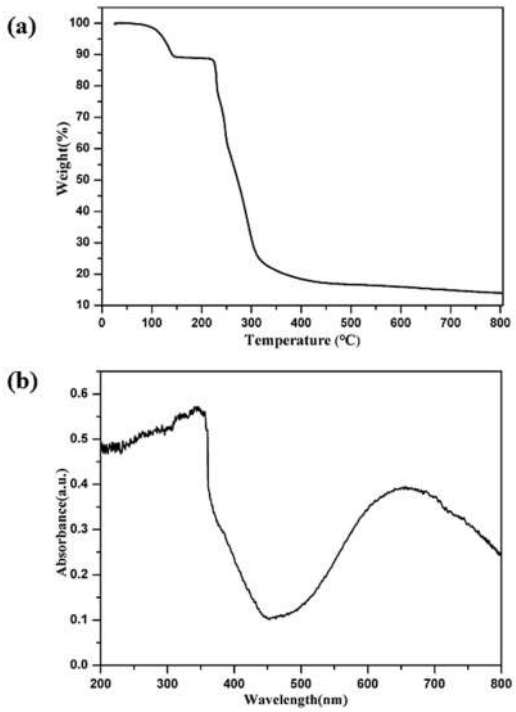

Figure 2. (a) The thermogravimetric curve of compound 1; (b) UV-Vis absorption spectra of **1**.

Table 3. π-π interactions for (Å, °) **1**.

Ring (I)···Ring (J)	Centroid to centroid distance (Å)	α (°)	Slippage distance (Å)
Cg3(N1/C1-C5)···Cg5(N3^{i}/C15^{i}-C16^{i}/C18^{i}-C20^{i})	3.849(2)	3.74(10)	1.912
Cg3(N1/C1-C5)···Cg5(N3^{ii}/C15^{ii}-C16^{ii}/C18^{ii}-C20^{ii})	3.933(2)	5.42(10)	1.915
Cg4(N2/C6-C10)···Cg4(N2^{iii}/C6^{iii}-C10^{iii})	3.855(2)	0.00(10)	1.796
Cg4(N2/C6-C10)···Cg8(N2^{iii}/C4^{iii}-C12^{iii})	3.7744(19)	0.83(8)	1.585
Cg5(N3/C15-C16/C18-C20)···Cg6(C4^{iv}-C6^{iv}/C10^{iv}-C12^{iv})	3.4993(19)	4.43(10)	1.033
Cg5(N3/C15-C16/C18-C20)···Cg7(N1^{iv}/C1^{iv}-C6^{iv}/C10^{iv}-C12^{iv})	3.5160(18)	4.63(8)	1.236
Cg5(N3/C15-C16/C18-C20)···Cg8(N2^{iv}/C4^{iv}-C12^{iv})	3.943(2)	4.60(8)	2.229
Cg5(N3/C15-C16/C18-C20)···Cg9(N1^{iv}-N2^{iv}/C1^{iv}-C12^{iv})	3.6668(19)	4.88(8)	1.713

Symmetry transformations used to generate equivalent atoms: ^{i} -*x*+2, -*y*, -*z*+1, ^{ii} *x*-1/2, -y+1/2, *z*+-1/2, ^{iii} -*x*+1, -*y*, -*z*+1, ^{iv} *x*+1/2,-*y*+1/2,*z*+1/2.

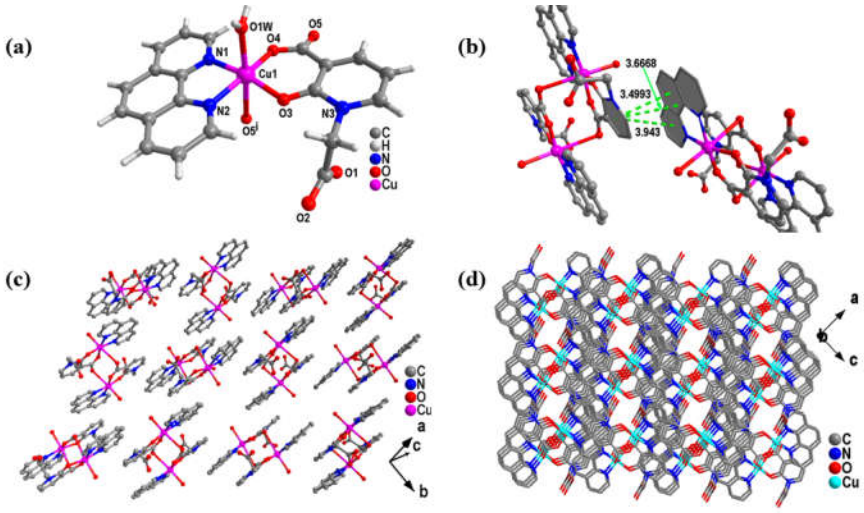

Figure 3. (a) Coordination environment of **1** (symmetry code: [i] -*x*+2, -*y*, -*z*+1**)**; (b) View of *π*-*π* interactions; (c) View of the 2D structure of **1**; (d) View of 3D supramolecular frameworks.

Hirshfeld surface analysis

The analysis of molecular crystal structures based on Hirshfeld surfaces was performed using CrystalExplorer 21.5 software [27-28]. Figure 4a reveals the Hirshfeld surface mapped over d_{norm} for **1**, where red surfaces indicate shorter contacts (less than the sum of the van der Waals VDW) radii), white scopes and blue regions denote contacts (tantamount to the sum of the VDW radii) and longer contacts (greater than the sum of the VDW radii), respectively. Figure 4a shows bright-red spots on d_{norm} made by hydrogen-bonding interactions between the O–H group of three waters and the oxygen atom of a carboxylate group and two crystal waters (Table 4). C–H···O interactions are likely designated by faint-red spots of the Hirshfeld surface. The two-dimensional fingerprint plots (FPP) were created and these are displayed with the corresponding percentage contribution (Figure 4c). The H···H, O···H/H···O and C···H/H···C intermolecular contacts have the total to percentage contribution of 87.9% in charge of the largest contributions for the crystal packing of **1**. C···C interactions have a percentage contribution of 8.3% and correspond mainly to *π*-*π* interactions in **1**. Significant *π*-*π* stacking interactions can be seen on the shape-index surface (Figure 4b), represented by red-yellow-blue-green triangles (and back-to-back rhombuses).

Table 4. H-Bonding geometry parameters (Å, °) for compound **1**.

D–H···A	D–H (Å)	H···A (Å)	D···A (Å)	D–H···A (°)
O(1W)-H(1A)···O(2)[v]	0.84	1.92	2.740(3)	164.5
O(1W)-H(1B)···O(3W)	0.84	1.97	2.794(3)	165.6
O(2W)-H(2A)···O(4)	0.85	2.58	3.188(2)	129.4
O(2W)-H(2A)···O(5)	0.85	2.03	2.861(3)	166.0
O(2W)-H(2B)···O(1)[i]	0.85	1.97	2.817(3)	177.7
O(3W)-H(3A)···O(2)[vi]	0.84	1.97	2.802(3)	170.9
O(3W)-H(3B)···O(2W)	0.85	2.02	2.855(3)	167.8

Symmetry transformations used to generate equivalent atoms: [i] -*x*+2, -*y*, -*z*+1, [v] -*x*+3/2, *y*+1/2, -*z*+3/2, [vi] *x*+1/2, -*y*+1/2, *z*-1/2.

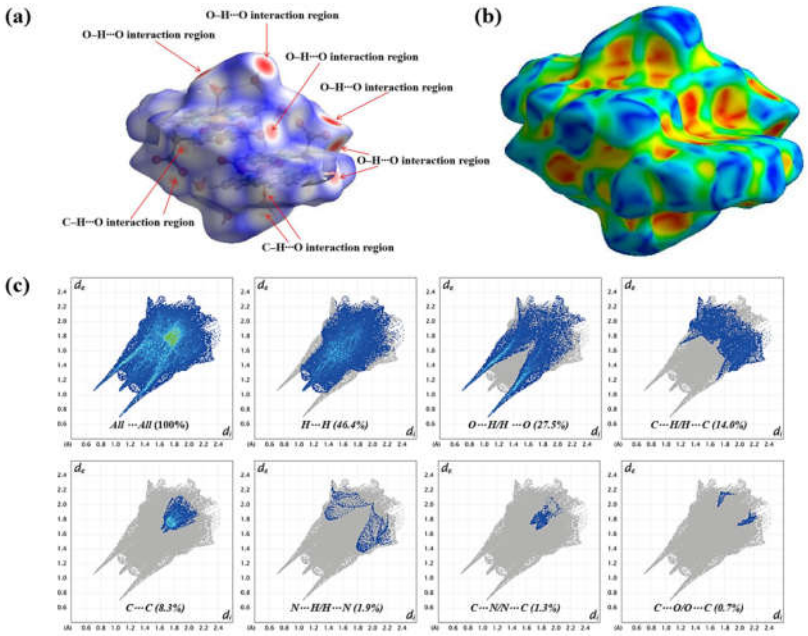

Figure 4. (a) View of the 3*D* Hirshfeld surface mapped of compound **1** over d_{norm}; (b) Hirshfeld surface evaluated over shape-index for **1**; (c) Two-dimensional fingerprint plots for the H···H, O···H/H···O, C···H/H···C, C···C, N···H/H···N, C···N/N···C, and C···O/O···C contacts of **1**.

DFT calculation

All calculations were implemented by the Gaussian09 program [29] with the structural parameters from the experimental data of **1**. Natural bond orbital (NBO) analysis [30] was executed by density functional theory (DFT) with the B3LYP [31] hybrid functional.

As shown in Table 5, the electronic configurations of Cu(II) ion, O and N atoms are $4s^{0.30}3d^{9.35}4p^{0.38}4d^{0.01}$, $2s^{1.64\sim1.72}2p^{4.95\sim5.04}3p^{0.01}$ and $2s^{1.34}2p^{4.16,4.17}3p^{0.02}$, respectively. The above results may concluded that the Cu(II) ion coordination with O and N atoms is mostly on the 4*s*, 3*d* and 4*p* orbitals, and O and N atoms mainly provide with electrons of 2*s* and 2*p* to the Cu(II) ion to form coordination bonds. On the basis of the valence-bond theory, the atomic net charge distribution in **1** state clearly covalent interactions between Cu(II) ion and the coordinated atoms.

In Figure 5, the HOMO and HOMO−1 are mainly composed of the π orbital of the **L** anions. The LUMO and HOMO−2 are made up mostly of the 3*d* orbital of Cu(II) ion, 2*p* orbitals of two N and four O atoms coordinated with Cu(II) ion. The LUMO+1 and LUMO+2 are mainly consist of the orbital of the phen ligands.

Table 5. Selected natural atomic charges and natural electron configuration of **1**.

Atom	Net charge	Electron configuration
Cu(1)	1.340	[core]4*s*(0.30)3*d*(9.35)4*p*(0.01)
O(3)	-0.743	[core]2*s*(1.69)2*p*(5.04)3*p*(0.01)
O(4)	-0.778	[core]2*s*(1.70)2*p*(5.06)3*p*(0.01)
O(1W)	-0.871	[core]2*s*(1.64)2*p*(5.22)3*p*(0.01)
O(5)^{i}	-0.675	[core]2*s*(1.72)2*p*(4.95)
N(1)	-0.532	[core]2*s*(1.34)2*p*(4.16)3*p*(0.02)
N(2)	-0.534	[core]2*s*(1.34)2*p*(4.17)3*p*(0.02)

Symmetry transformations used to generate equivalent atoms: ^{i} -*x*+2, -*y*, -*z*+1.

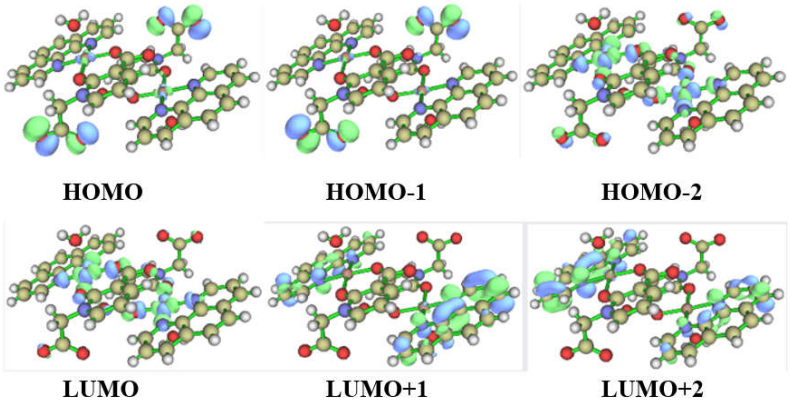

Figure 5. Frontier molecular orbitals of **1**.

CONCLUSION

In summary, by using 3-carboxy-1-carboxymethyl-2-oxidopyridinium with phen ligand, novel Cu(II) coordination compound, $[Cu(L)_2(phen)_2(H_2O)_2]\cdot 4H_2O$ (**1**) was obtained. $[Cu_2(L)_2(phen)_2(H_2O)_2]\cdot 4H_2O$ linked by *π*-*π* interactions to form 2*D* supramolecular layer, which eventually extended into more stable 3*D* architecture through hydrogen bonds and *π*-*π* interactions. Hirshfeld surface analysis of **1** was performed along with the calculation of two-dimensional fingerprint plots to gain further understanding of the intermolecular interactions within the crystal. This analysis showed that the interactions of H···H (46.4%), O···H/H···O (27.5%) and C···H/H···C (14.0%) interactions are dominant. And DFT calculations have also been carried out.

ACKNOWLEGDEMENTS

This work was supported by the Natural Science Fund Program of Jilin Province (No. 20240101148JC).

Supplementary data

Crystallographic data have been deposited with the Cambridge Crystallographic Data Centre as supplementary publication number CCDC 2335195. Copies of this information may be obtained

free of charge from The Director, CCDC, 12 Union Road, Cambridge, CB2 1EZ, UK (fax: +44-1223-336033; email: deposit@ccdc.cam.ac.uk or www: http://www.ccdc.cam.ac.uk).

REFERENCES

1. Ding, B.; Wu, J.; Wu, X.X.; Huo, J.Z.; Zhu, Z.Z.; Liu, Y.Y.; Shi, F.X. Syntheses, structural diversities and characterization of a series of coordination polymers with two isomeric oxadiazol-pyridine ligands. *RSC Adv*. **2017**, 7, 9704-9718.
2. Weng, Z.H.; Liu, D.C.; Chen, Z.L.; Zou, H.H.; Qin, S.N.; Liang, F.P. Two types of lanthanide coordination polymers of (2,3-f)-pyrazino(1,10)phenanthroline-2,3-dicarboxylic acid: Syntheses, structures, and properties. C*ryst. Growth Des.* **2009**, 9, 4163-4170.
3. Yu, C.Y.; Li, H.; Luo, J.W.; Zheng, M.K.; Zhong, W.B.; Yang, W.T. Metal-organic coordination polymer/multi-walled carbon nanotubes composites to prepare N-doped hierarchical porous carbon for high performance supercapacitors. *Electrochim. Acta* **2018**, 284, 69-79.
4. Feng, J.D.; Song,Y.Z.; Wang, X.Y.; Yu. Y.; Liu, J.X. N-ligands mediated Co(II) coordinattion polymer incorpoprating 5-hydroxyisophthalic acid :syntheses ,structures, and theoretical calculations. *Bull. Chem. Soc. Ethiop*. **2024**, 38, 877-887.
5. Li, S.; Wang, B.Q.; Liu, G.C.; Li, X.H.; Sun, C.; Zhang, Z.; Wang. X.L. Achieving ultra-trace analysis and multi-light driven photodegradation toward phenolic derivatives via a bifunctional catalyst derived from a Cu(I)-complex-modified polyoxometalate. *Inorg. Chem. Front.* **2024**, 11, 1561-1572.
6. Wang, X.P.; Li, M.L.; Zhang, J.; He, X.H.; Crittenden, J.C.; Zhang, W. Silver ion-exchanged anionic metal−organic frameworks for iodine adsorption: Silver species evolution from ions to nanoparticles. *ACS Appl. Nano Mater*. **2023**, 6, 7206-7217.
7. Derafa, W.; Elkanzi, N.A.A.; Ali, A.M.; Abdou, A. Three Co(II), Ni(II) and Cu(II) Schiff base complexes incorporating 2-[(4-{[(4-methylphenyl)sulfonothioyl]oxy}phenyl)methylene] amino}benzoic acid: Synthesis, structural, DFT, biological and molecular docking investigation. *Bull. Chem. Soc. Ethiop.* **2024**, 38, 325-346.
8. Chen, W.; Fan, R.Q.; Zhang, H.J.; Dong, Y.W.; Wang, P.; Yang, Y.L. Tunable white-light emission PMMA-supported f ilm materials containing lanthanide coordination polymers: preparation, characterization, and properties. *Dalton Trans.* **2017**, 46, 4265-4277
9. Wang, H.L.; Wang, X.; Li, M.M.; Feng, J.D. Two new Zn(II) coordination polymers incorporating 2-(2,6-dichlorophenyl)-1H-imidazo[4,5-f][1,10]phenanthroline: Synthesis and structure. *Main Group Met. Chem.* **2024**, 47, 20230033.
10. Naskar, S.; Pakhira, B.; Mishra, D.; Mitra, P.; Chattopadhyay, S.K.; Naskar, S. Synthesis, characterization and theoretical studies of the heteroleptic ruthenium(II) complexes of 2,6-bis(benzimidazolyl)pyridine. *Polyhedron* **2015**, 100, 170-179.
11. Zhang, X.; Zhuang, X.R.; Zhang, N.X.; Ge, C.Y.; Luo, X.; Li, J.X.; Wu, J.; Yang, Q.; Liu, R. A luminescent sensor based on Zn(II) coordination polymer behave selective and sensitive detection for NACs and Fe^{3+} ions. *Cryst. Eng. Comm*. **2019**, 21, 1948-1955.
12. Li, L.; Liu, C.B.; Yang, G.S.; Xiong, Z Q.; Liu, H.; Wen, H.L. Zn(II) coordination polymers with flexible V shaped dicarboxylate ligand: Syntheses, helical structures and properties. *J. Solid State Chem.* **2015**, 231, 70-79.
13. Siebert, R.; Tian, Y.X.; Camacho, R.; Winter, A.; Wild, A.; Krieg, A.; Schubert, U.S.; Popp, J.; Scheblykin, I.G.; Dietzek, B. Fluorescence quenching in Zn^{2+}-bis-terpyridine coordination polymers: a single molecule study. *J. Mater. Chem.* **2012**, 22, 16041-16050.
14. Ma, D.Y.; Guo, H.F.; Dong, J.; Xu, J. Unusual self-assembled 1D tape of tetramers and water–nitrate clusters trapped in a zinc(II) complex: Synthesis,characterization, luminescence and catalytic properties. *J. Mol. Struct.* **2013**, 1054-1055, 46-52.

15. Yu, M.H.; Hu, M.; Wu, Z.T.; Su, H.Q. Syntheses, crystal structures and properties of five divalent transition metal coordination compounds based on a semirigid tetracarboxylic acid ligand. *Inorg Chim. Acta* **2013**, 408, 84-90.
16. Wang, K.; Wang, H.L.; Bian, Y.Z.; Li, W.J. Zn(II) metal-organic frameworks (MOFs) assembled from semirigid multicarboxylate ligands: Synthesis, crystal structures, and luminescent properties. *Solid State Sci*. **2010**, 12, 1791-1796.
17. Yadav, P.K.; Kumari, N.; Pachfule, P.; Banerjee, R.; Mishra, L. Metal [Zn(II), Cd(II)], 1,10-phenanthroline containing coordination polymers constructed on the skeleton of polycarboxylates: synthesis, characterization, microstructural, and CO_2 gas adsorption studies. *Cryst. Growth Des.* **2012**, 12, 5311-5319;.
18. Song, Y.Z.; Li, W.; Jin, R.W.; Feng, J.D. Syntheses, structures, and characterization of two new Zn(II)/Cd(II) complexes with phenanthroline derivative. *Main Group Met. Chem.* **2024**, 47, 20240009.
19. Yang, Y.Q.; Yang, J.; Kan, W.Q.; Yang, Y.; Guo, J.; Ma, J.F. A series of 1D, 2D, and 3D coordination polymers based on flexible 3-carboxy-1-carboxymethyl-2 oxidopyridinium and different N-donor ligands syntheses, structures, and luminescent properties. *Eur. J. Inorg. Chem.* **2013**, 2013, 280-292.
20. Nie, F.; Yu, R.; Wang, L.N.; Jiang, L.P.; Wu, Q.; Xu, W.H.; Fu, X.L. Electrochemiluminescence properties and sensing application of Zn(II)−metal−organic frameworks constructed by mixed ligands of para dicarboxylic acids and 1,10-phenanthroline. *ACS Omega* **2023**, 8, 43463-43473.
21. Jaros, S.W.; Sokolnicki, J.; Siczek, M.; Smoleński, P. Strategy for an effective eco-optimized design of heteroleptic Cu(I) coordination polymers exhibiting thermally activated delayed fluorescence. *Inorg. Chem.* **2023**, 62, 19898-19907.
22. Bendjellal, N.; Trifa, C.; Bouacida, S.; Boudaren, C.; Boudraa, M.; Merazig, H. Two novel alkaline earth coordination polymers constructed from cinnamic acid and 1,10-phen anthroline: Synthesis and structural and thermal properties. *Acta Crystallogr. C* **2018**, 74, 240-247.
23. He, D.F.; Liu, S.M.; Zhou F.J.; Zhao X.J.; Liu, Y.W.; Fang L.; Liu S.X. Recognition of trace organic pollutant and toxic metal ions via a tailored fluorescent metal–organic coordination polymer in water environment. *RSC Adv.* **2018**, 8, 34712.
24. Burla, M.C.; Caliandro, R.; Carrozzini, B.; Cascarano, G.L.; Cuocci, C.; Giacovazzo, C.; Mallamo, M.; Mazzone, A.; Polidori, G. Crystal structure determination and refinement via SIR2014. *J. Appl. Crystallogr*. **2015**, 48, 306-309.
25. Sheldrick, G.M. Crystal structure refinement with SHELXL. *Acta Crystallogr. C* **2015**, 71, 3-8.
26. Zhao, L.Y.; Deng, X.C.; Gao, J.; Ma Y.J. Studying of the structure diverse and photocatalytic activities of two 1,4-bis (imidazole-1-methyl)-benzene-based coordination polymers. *Inorg Chim Acta* **2023**, 544, 121227.
27. Spackman, P.R.; Turner, M.J.; McKinnon, J.J.; Wolff, S.K.; Grimwood, D.J.; Jayatilaka, D.; Spackman, M.A. CrystalExplorer: A program for Hirshfeld surface analysis, visualization and quantitative analysis of molecular crystals. *J. Appl. Cryst.* **2021**, 54, 1006-1011.
28. McKinnon, J.J.; Jayatilaka, D.; Spackman, M.A. Towards quantitative analysis of intermolecular interactions with Hirshfeld surface. *Chem. Commun.* **2007**, 37, 3814-3816.
29. Frisch, M.J.; Trucks, G.W.; Schlegel, H.B.; Scuseria, G.E.; Robb, M.A.; Cheeseman, J.R.; Fox, D.J. *Gaussian 09, Rev*. Gaussian Inc: Wallingford; **2009**.
30. Reed, A.E.; Curtiss, L.A.; Weinhold, F. Intermolecular interactions from a natural bond orbital, donor-acceptor viewpoint. *Chem. Rev*. **1988**, 88, 899-926.
31. Lee, C.; Yang, W.; Parr, R.G. Development of the Colle-Salvetti correlation-energy formula into a functional of the electron density. *Phys. Rev. B* **1988**, 37, 785-789.